Molecular Magnets

DOI: 10.1002/ange.200501265

Phosphonate Ligands Stabilize Mixed-Valent $\{Mn^{III}_{20-x}Mn^{II}_{x}\}$ Clusters with Large Spin and Coercivity**

Shanmugam Maheswaran, Guillaume Chastanet, Simon J. Teat, Talal Mallah, Roberta Sessoli, Wolfgang Wernsdorfer, and Richard E. P. Winpenny**

The discovery that some molecules show a slow relaxation of magnetization below a critical temperature has prompted a large interest in the materials now generally known as "single molecule magnets" (SMMs).[1,2] Investigations have been inspired partly by the idea that SMMs could be used as molecular magnetic storage devices but also because they show unusual phenomena such as quantum-tunneling of magnetization,[3] which can be exchange-biased.[4] The majority of SMMs have been made by Christou and co-workers, and contain Mn^{III} ions;[5–7] the use of Mn^{III} ions has significant advantages as cages containing this ion often have ground states with large spin values and considerable anisotropy derived from the Jahn–Teller distortion common to a d^4 ion.

Phosphonates, such as benzylphosphonate ($PhCH_2PO_3^{2-}$), have only rarely been employed in making transition-metal cages, probably because of the insolubility of metal phosphonates. Recently we showed that the reaction of phosphonates

[*] Dr. G. Chastanet, Prof. R. Sessoli
Laboratorio di Magnetismo Molecolare
Dipartimento di Chimica
Università degli Studi di Firenze & INSTM
Via della Lastruccia n. 3, 50019 Sesto Fiorentino (Italy)
Fax: (+39) 055-457-3372
E-mail: roberta.sessoli@unifi.it

S. Maheswaran, Prof. R. E. P. Winpenny
University of Manchester
School of Chemistry
Oxford Road, Manchester, M13 9PL (UK)
Fax: (+44) 161-275-4616
E-mail: richard.winpenny@manchester.ac.uk

Dr. S. J. Teat
CCLRC Daresbury Laboratory
Warrington, Cheshire, WA4 4AD (UK)

Prof. T. Mallah
Laboratoire de Chimie Inorganique
UMR CNRS 8613, Université Paris Sud
91405 Orsay (France)

Dr. W. Wernsdorfer
Laboratoire Louis Néel–CNRS, BP 166
25 Avenue des Martyrs, 38042 GRENOBLE Cedex 9 (France)

[**] This work was supported by the EC-TMR Network "QuEMolNa" (MRTN-CT-2003-504880), the ORS (UK), the University of Manchester, the "Deutsche Forschungsgemeinschaft" (SPP1137), and Italian MIUR (for FIRB and PRIN funding). S.M. thanks EST, FP6-504204: MOLMAG for supporting a study period in Florence.

Supporting information for this article is available on the WWW under http://www.angewandte.org or from the author.

with preformed trinuclear iron–carboxylate clusters generates a range of new polymetallic complexes.[8] In our search for new SMMs we have extended this work to mixed-valent basic manganese carboxylates such as $[Mn_3O(O_2CR)_6(py)_3]$ (py = pyridyl).

Reaction of equimolar amounts of $H_2O_3PCH_2Ph$ and $[Mn_3O(O_2CCMe_3)_6(py)_3]$ in CH_3CN in the presence of Et_3N gave a dark brown solution from which $[Et_3NH]_2[Mn^{III}_{18}Mn^{II}_2(\mu_4\text{-}O)_8(\mu_3\text{-}O)_4(\mu_3\text{-}OH)_2(O_3PCH_2Ph)_{12}(O_2CCMe_3)_{10}(py)_2]$ (**1**) crystallizes in 40% yield after two days. Structural analysis[9] shows that the μ_3-oxo-centered triangular array of manganese centers in the precursor cage is maintained in the product (for example: Mn1, Mn2, Mn3, and symmetry equivalents; Figure 1); however, **1** is best described as a centrosymmetric cubic-close packed array of Mn sites. Twelve of the manganese centers lie in one plane, which includes the two Mn^{II} sites (Mn6 and Mn6a in Figure 1). Two Mn^{III} triangles (Mn5, Mn8, and Mn10, and the symmetry related ions) lie above and below hexagons of Mn in the central plane and bridged to the central layer by a μ_4-oxide group (Figure 1b). The relative orientation of the two triangles makes the packing ABC, not ABA, hence this is a fragment of a cubic close-packed (ccp) lattice (see Figure 1b). Mn1 lies in the outer plane containing the triangle formed by Mn5, Mn8, and Mn10, and forms a μ_3-oxo-centered triangle with two ions of the central plane (Mn2 and Mn3). The Mn^{II} site is seven-coordinate, while all the Mn^{III} sites are six-coordinate with Jahn–Teller elongations. Valence bond sum analysis confirms the oxidation states, as well as the assignment of two hydroxide and twelve oxide bridges. The Et_3NH cations hydrogen bond to O atoms from phosphonate groups (N–H···O(phos) 2.78 Å). The twelve phosphonate ligands in **1** show three bonding modes: 3.111, 4.211, and 5.221 (Harris notation[8]), with four examples of each mode in the structure.

Two related clusters can be made from mixed-valent $[Mn_3O(O_2CPh)_6(py)_2(H_2O)]$ and homovalent $[Mn_3O(O_2CPh)_6(py)_3]ClO_4$ benzoate triangles: $K_4[Mn^{III}_{16}Mn^{II}_4(\mu_4\text{-}O)_4(\mu_3\text{-}O)_6(PhCH_2PO_3)_{14}(PhCO_2)_{12}(PhCO_2H)_{0.5}(CH_3CN)_2]$ (**2**) and $Na_6[Mn^{III}_{14}Mn^{II}_6(\mu_4\text{-}O)_4(\mu_3\text{-}O)_4(OH)_4(PhCH_2PO_3)_{14}(PhCO_2)_{12}(PhCO_2H)_2(H_2O)_4(CH_3CN)_4]$ (**3**) can be formed, depending on whether K^I or Na^I ions are present. The manganese cores are similar to that in **1**, and the center of symmetry is retained; however, additional Mn^{II} sites are found within the central layer. Mn4 in **2** has been assigned as being in the Mn^{II} oxidation state because of an increase in the average bond length to 2.163 Å (from 2.011 Å in **1**), while the other Mn–O bond lengths remain virtually unchanged. The average bond length to Mn4 in **3** remains long (2.184 Å), but a significant increase is also observed around Mn7 (2.140 Å compared to 2.023 Å for **1** and 2.022 Å for **2**). Mn4 and Mn7 in **3** are thus assigned as Mn^{II} sites. The alkali-metal cations are attached to the periphery of the cages and have no structure-directing role. This result allows us to isolate three different redox states of mixed-valent cages with the same high nuclearity.

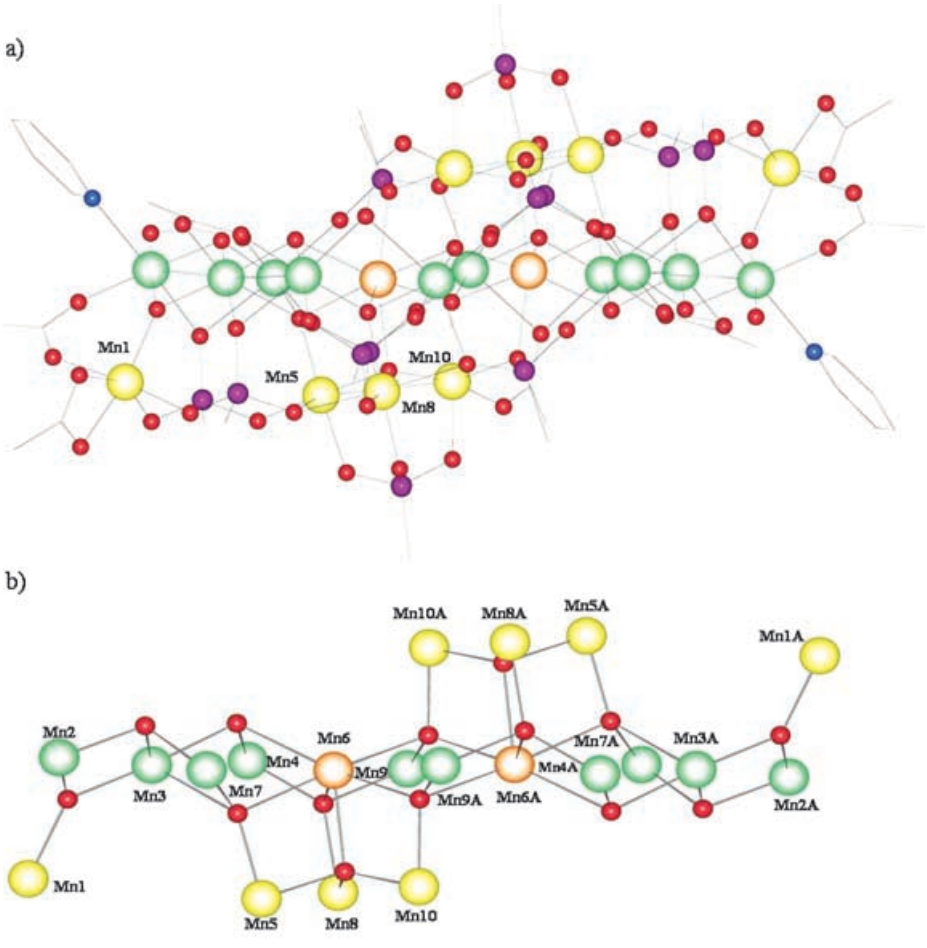

Figure 1. The structure of **1** in the crystal: a) viewed parallel to the central Mn plane (the H and C atoms of the organic side-chains are omitted for clarity), color code: green and yellow, Mn^{III}; orange, Mn^{II}; magenta, P; red, O; blue, N; b) view parallel to the central plane showing the ABC packing of the Mn ions and the bridging oxygen atoms.

The variable-temperature direct current (dc) magnetic susceptibilities measured for the three compounds are shown in Figure 2a. All three compounds show the same type of behavior: the χT value increases from nearly 60 (**1**) and 68 emu K mol^{-1} (**2** and **3**) at room temperature to reach maxima of 210 (**1**), 115 (**2**), and 74 emu K mol^{-1} (**3**). A rapid decrease is observed around 10 K which probably results from zero-field splitting or intermolecular interactions. These curves suggest the three cages have a high-spin ground state: $S = 19 \pm 1$ for **1**, $S =$

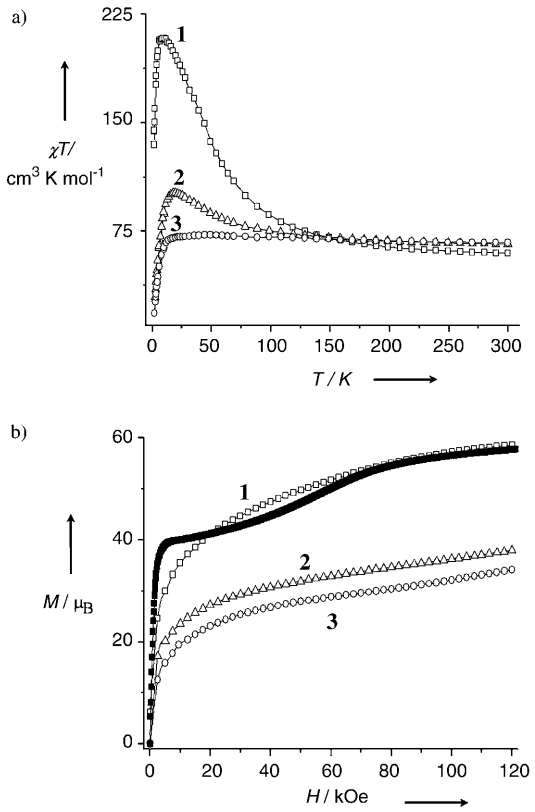

Figure 2. a) Temperature-dependence of the χT value for a polycrystalline sample of **1**, **2**, and **3**; b) magnetization versus field data for **1**, **2**, and **3** recorded at 1.55 K. The filled squares represent the single-crystal magnetization of **1** along the easy axis.

14 ± 1 for **2**, and $S = 11 \pm 1$ for **3**. The magnetization (M) versus magnetic field (H) data are in agreement with the χT plots, and further confirm the large spin values of the ground states. Magnetization measurements were performed on polycrystalline samples at 1.55 K to determine the ground state more accurately (Figure 2b). A two-step curve is obtained for all three compounds, with first a rapid saturation around 40 μ_B (**1**), 30 μ_B (**2**), and 25 μ_B (**3**), followed by a slow increase in the value of M. Single-crystal magnetization measurements performed along the easy axis of the cluster **1** show a pronounced saturation around 40 μ_B at low field, followed by a broad step (Figure 2b).

The further increase in the magnetization is consistent with the presence of excited states close in energy that have a larger spin value. This observation is not surprising when Mn^{II} ions are present as they often lead to weak antiferromagnetic exchange interactions, which can easily be overcome by an external magnetic field. The observed difference in the single-crystal and powder data for **1** suggests that it has a significant magnetic anisotropy which when associated with the large S value ($S = 19 \pm 1$) could lead to slow relaxation of the magnetization.

Alternating current (ac) susceptibility measurements in zero field allows estimation of the energy barrier for the reorientation of the magnetization of superparamagnetic particles or molecules functioning as SMMs.[2] The applied oscillating field probes the dynamics of this reorientation, as the out-of-phase signal (χ'') is maximal when the frequency of the ac field equals the relaxation rate of the magnetization. We monitored the value of χ'' from 1.5 to 10 K at several frequencies between 100 to 20000 Hz. Maxima were observed for compounds **1** and **2** (the data for **1** are shown in Figure 3).

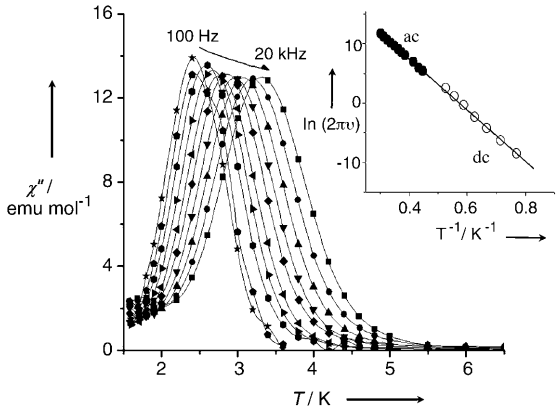

Figure 3. Temperature-dependence of the out-of-phase susceptibility of **1** measured from 100 to 20000 Hz. Inset: the temperature-dependence of the relaxation time extracted from ac measurements and time decay of the magnetization.

In contrast, only a frequency-dependent increase in the value of χ", with no maxima down to 1.5 K, has been observed for **3**. The energy barrier for the relaxation can be derived from the Arrhenius plot[2c] as 43 K ($\tau_0 = 2 \times 10^{-11}$ s) for **1** and 17 K ($\tau_0 = 2 \times 10^{-10}$ s) for **2**, with a moderate distribution of relaxation times. All three compounds are therefore new SMMs, and **1** possesses one of the highest energy barriers known after $\{Mn_{12}\}$ clusters.[2a] It is also one of the highest spin SMMs known.[6,10] It is worth noting that the energy barrier increases from **3** to **1** as the content of anisotropic Mn^{III} ions and the ground spin state of the cluster increases.

The decay of remnant magnetization (see Supporting Information) has been followed on a microcrystal of **1** with a micro-Squid[11] and the relaxation time—extracted as the time delay at which M/M_0 equals $1/e$—is in good agreement with the values extracted from ac measurements (see inset of Figure 3). A square hysteresis loop has been measured that widens on lowering the temperature, with a remarkably high coercive field of 10 kOe below 0.4 K (Figure 4). Previously reported large Mn cages have much narrower hysteresis loops.[6,7] No sudden jumps at $H = 0$ are observed here, which suggests resonant quantum tunneling is not particularly efficient. This proposal is confirmed by the unchanged value of the relaxation time τ extracted from ac susceptibility measurements in zero and under moderate static fields. The shape of the hysteresis is unusual, as it shows small steps around 4 and 9 kOe on the descending field branch. A detailed analysis of the hysteretic behavior of these steps shows that they are not related to dynamic properties but rather that they correspond to a cross-over to a magnetic ground state of higher S value that is induced by the applied field.[12]

The $S = 19 \pm 1$ ground state of **1** in low field can be tentatively rationalized as follows. The strongest antiferro-

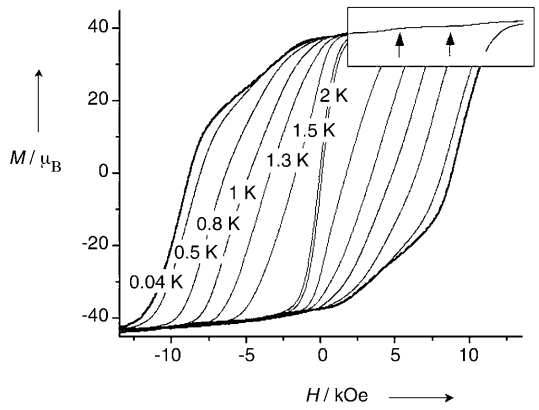

Figure 4. Hysteresis loops measured at a sweep rate of 350 Oe s^{-1} on a crystal of **1** at different temperatures. Steps at 4 and 9 kOe are indicated by arrows.

magnetic interactions are likely to result from μ_3-oxides which are all associated with the triangle Mn1-Mn2-Mn3 and its symmetry equivalent. We assume that these triangles are spin-frustrated and have a low resulting spin.[13]

We can then consider the remaining twelve Mn^{III} and two Mn^{II} sites in the structure; the Mn^{III} sites are bridged by μ_4-oxide and μ_3-hydroxide groups, which can often create ferromagnetic exchange. In contrast, exchange between Mn^{II} and Mn^{III} sites in similar structures is often weak and antiferromagnetic. We can thus propose that the spin of the ground state at low field arises as a consequence of the spin of the twelve Mn^{III} ions ($S = 24$) opposed to the spin of the two Mn^{II} ions ($S = 5$) plus the contribution from the two frustrated triangles. The large change in the ground state S value would then result from the field overcoming the antiferromagnetic exchange between the Mn^{III} and Mn^{II} ions, thus leading to an increase in the S value of 10 and in the M value of 20 μ_B. The observed decrease in the value of S on reduction of Mn^{III} to Mn^{II} confirms the proposed picture, in which the antiparallel aligned spins are associated with Mn^{II} sites. This oversimplified model would, however, predict changes in S of 9 and 18 in going from **1** to **2** and **3**, respectively. The smaller difference observed suggests a more complicated scenario where intermediate spin states are stabilized by competing antiferromagnetic interactions. X-ray magnetic circular dichroism, which is able to distinguish how the two oxidation states contribute to the magnetic moment, thus seems the appropriate technique to investigate the spin structure of these compounds.

The three compounds are therefore very unusual SMMs as shown by the very high spin and high coercivity of **1**, in the immediate availability of three redox forms of the cluster, and finally the observation of a dramatic change in the spin of the ground state.

Experimental Section

All reagents were used as received from Aldrich. $[Mn_3O(O_2CCMe_3)_6(py)_3]$, $[Mn_3O(PhCO_2)_6(py)_2(H_2O)]$, and $[Mn_3O(PhCO_2)_6(py)_3]$ ClO_4 were made by literature procedures.[14]

1: A brown solution of $[Mn_3O(O_2CCMe_3)_6(py)_3]$ (0.58 g, 0.56 mmol) in MeCN (10 mL) was treated with $PhCH_2PO_3H_2$ (0.096 g, 0.56 mmol) and triethylamine (0.14 mL). The resulting solution was stirred for 15 h and then filtered. Very large crystals grew from the filtrate after two days. The crystals were suitable for X-ray studies. Yield: 0.24 g (40 %). Elemental analysis calcd (%) for $C_{156}H_{218}Mn_{20}N_4O_{70}P_{12}\cdot 2\,CH_3CN$: C 39.85, H 4.68, N 1.74, P 7.71; found: C 39.12, H 4.75, N 2.09, 7.73.

2: $[Mn_3O(PhCO_2)_6(py)_2(H_2O)]$ (0.54 g, 0.5 mmol) and $PhCH_2PO_3$ (0.086 g, 0.5 mmol) were mixed in a CH_3CN/EtOH (5:1) mixture (12 mL), and KOMe (0.035 g, 0.5 mmol) was added. The solution was stirred overnight and filtered. Crystals of **2** grew from the filtrate after three days. Yield: 0.21 g (60 %). Elemental analysis (%) calcd for $C_{189.5}H_{167}Mn_{20}N_2K_4O_{77}P_{14}$ (dried): C 42.50, H 3.12, N 0.51, P 8.04; found: C 42.63, H 3.41, N 0.22, P 7.76.

3: $[Mn_3O(PhCO_2)_6(py)_3]ClO_4$ (0.59 g, 0.5 mmol), $PhCH_2PO_3H_2$ (0.086 g, 0.5 mmol), and Et_3N (0.14 mL) were mixed in CH_3CN (10 mL) and the solution stirred for 15 h before being filtered. A solution of $NaClO_4$ (0.24 g) in CH_3CN (2–3 mL) was added to the filtrate and the mixture again filtered before keeping the filtrate for crystallization. After two days dark brown single crystals of **3** grew that were suitable for X-ray analysis. Yield: 0.15 g (30 %). Elemental analysis calcd (%) for $C_{204}H_{194}Mn_{20}N_4Na_6O_{86}P_{14}$ (dried) : C 42.61, H 3.40, N 0.98, P 7.54; found: C 42.98, H 3.81, N 0.98, P 7.72.

Magnetic measurements: The temperature-dependence of the magnetization was measured on polycrystalline powder samples with a Cryogenic S600 SQUID magnetometer at 10 kOe and below 50 K at 1 kOe to avoid saturation. Data have been corrected for the diamagnetic contribution according to Pascal tables. Magnetization curves up to 120 kOe have been obtained by using an Oxford Instruments Vibrating Sample Magnetometer (VSM). Alternating current susceptibility data were obtained by using a home-made probe[15] with an oscillating field of 0.8 Oe. A home-made μ-SQUID magnetometer[11] was used for low-temperature magnetic measurements on single microcrystals of **1**.

Received: April 11, 2005
Published online: July 20, 2005

Keywords: cluster compounds · magnetic properties · manganese · molecular magnets · spin crossover

[1] A. Caneschi, D. Gatteschi, R. Sessoli, A. L. Barra, L. C. Brunel, M. Guillot, *J. Am. Chem. Soc.* **1991**, *113*, 5873–5874.
[2] a) R. Sessoli, H.-L. Tsai, A. R. Schake, S. Wang, J. B. Vincent, K. Folting, D. Gatteschi, G. Christou, D. N. Hendrickson, *J. Am. Chem. Soc.* **1993**, *115*, 1804–1816; b) R. Sessoli, D. Gatteschi, A. Caneschi, M. A. Novak, *Nature* **1993**, *365*, 141–143; c) D. Gatteschi, R. Sessoli, *Angew. Chem.* **2003**, *115*, 278–309; *Angew. Chem. Int. Ed.* **2003**, *42*, 268–297, and references therein.
[3] a) J. R. Friedman, M. P. Sarachik, J. Tejada, R. Ziolo, *Phys. Rev. Lett.* **1996**, *76*, 3830–3833; b) L. Thomas, F. Lionti, R. Ballou, D. Gatteschi, R. Sessoli, B. Barbara, *Nature* **1996**, *383*, 145–147.
[4] W. Wernsdorfer, N. Aliaga-Acaldse, D. N. Hendrickson, G. Christou, *Nature* **2002**, *416*, 406–409.
[5] E. K. Brechin, C. Boskovic, W. Wernsdorfer, J. Yoo, A. Yamaguchi, E. C. Sanudo, T. R. Concolino, A. Rheingold, H. Ishimoto, D. N. Hendrickson, G. Christou, *J. Am. Chem. Soc.* **2002**, *124*, 9710–9711, and references therein.
[6] M. Murugesu, M. Habrych, W. Wernsdorfer, K. A. Abboud, G. Christou, *J. Am. Chem. Soc.* **2004**, *126*, 4766–4767.
[7] A. Tasiopoulos, A. Vinslava, W. Wernsdorfer, K. A. Abboud, G. Christou, *Angew. Chem.* **2004**, *116*, 2169–2173; *Angew. Chem. Int. Ed.* **2004**, *43*, 2117–2121.

[8] E. I. Tolis, M. Helliwell, S. Langley, J. Raftery, R. E. P. Winpenny, *Angew. Chem.* **2003**, *115*, 3934 – 3938; *Angew. Chem. Int. Ed.* **2003**, *42*, 3804 – 3808.

[9] Crystal data for **1**·10 MeCN: $C_{176}H_{240}Mn_{20}N_{14}O_{70}P_{12}$, $M_r = 5142.26\ g\,mol^{-1}$, small brown block, monoclinic, space group $P2_1/c$, $a = 15.9789(15)$, $b = 26.171(2)$, $c = 29.955(3)$ Å, $\beta = 121.131(6)°$, $V = 10722.9(17)$ Å^3, $Z = 2$ (the molecule lies on an inversion centre), $T = 100(2)$ K, $\rho_{calcd} = 1.593\ g\,cm^{-1}$, $F(000) = 5268$, $\mu(Mo_{K\alpha}) = 1.306\ mm^{-1}$. Crystal data for **2**: $C_{189.5}H_{167}Mn_{20}N_2K_4O_{77}P_{14}$, dark brown block, triclinic, space group $P\bar{1}$, $a = 17.3198(13)$, $b = 18.7550(14)$, $c = 20.4374(15)$ Å, $\alpha = 80.494(10)$, $\beta = 82.255(10)$, $\gamma = 81.169(10)°$, $V = 6429.1(8)$ Å^3, $Z = 1$ (the molecule lies on an inversion centre), $T = 100.0(2)$ K, $\rho_{calcd} = 1.447\ g\,cm^{-1}$, $F(000) = 2828$, $\mu(MoK_\alpha) = 1.174\ mm^{-1}$. Crystal data for **3**: $C_{204}H_{194}Mn_{20}N_4Na_6O_{86}P_{14}$, dark brown plate, triclinic, space group $P\bar{1}$, $a = 16.166(3)$, $b = 20.360(4)$ $c = 22.781(5)$ Å, $\alpha = 68.97(19)°$, $\beta = 71.69(2)°$, $\gamma = 77.051(16)°$, $V = 6592(2)$ Å^3, $Z = 1$ (the molecule lies on an inversion centre), $T = 100.0(2)$ K, $\rho_{calcd} = 1.577\ g\,cm^{-1}$, $F(000) = 3178$, $\mu(Mo_{K\alpha}) = 1.104\ mm^{-1}$. Data were collected on a Bruker SMART CCD diffractometer ($Mo_{K\alpha}$, $\lambda = 0.71073$). In all cases the selected crystals were mounted on the tip of a glass pin using paratone-N oil and placed in the cold flow (100 K) produced with an Oxford cryocooling device. Complete hemispheres of data were collected using ω scans (0.3°, 30 seconds per frame). Integrated intensities were obtained with SAINT+ [16] and they were corrected for absorption using SADABS.[16] Structure solution and refinement was performed with the SHELX package.[16] The structures were solved by direct methods and completed by iterative cycles of ΔF syntheses and full-matrix least-squares refinement against F^2 to give: for **1**: using 1321 parameters and 98 restraints, $wR_2 = 0.2260$ (12935 unique reflections), $R_1 = 0.1033$ (11281 reflections with $I > 2\sigma(I)$); for **2:** using 1397 parameters and 478 restraints, $wR_2 = 0.2206$ (20413 unique reflections), $R_1 = 0.0611$ (17353 reflections with $I > 2\sigma(I)$); for **3**: using 1608 parameters without restraints, $wR_2 = 0.2626$ (7978 unique reflections), $R_1 = 0.0893$ (7306 reflections with $I > 2\sigma(I)$). CCDC-268450–268452 contain the supplementary crystallographic data for this paper. These data can be obtained free of charge from the Cambridge Crystallographic Data Centre via www.ccdc.cam.ac.uk/data_request/cif.

[10] J. Lorionova, M. Gross, M. Pilkington, H. Andres, H. S. Evans, H. U. Gudel, S. Decurtins, *Angew. Chem.* **2000**, *112*, 1667 – 1672; *Angew. Chem. Int. Ed.* **2000**, *39*, 1605 – 1609.

[11] W. Wernsdorfer, *Adv. Chem. Phys.* **2001**, *118*, 99 – 192.

[12] K. L. Taft, C. D. Delfs, G. C. Papaefthymiou, S. Foner, D. Gatteschi, S. J. Lippard, *J. Am. Chem. Soc.* **1994**, *116*, 823 – 832.

[13] An isosceles triangle of antiferromagnetically coupled $S = 2$ spins described by the spin Hamiltonian $\mathscr{H} = J(\mathbf{S_1S_2}+\mathbf{S_1S_3}) + J'(\mathbf{S_2S_3})$ has $S = 0$ ground state if J'/J is between 2/3 and 3/2. The reduction in the symmetry and the introduction of a third coupling constant does not significantly alter this picture.

[14] J. B. Vincent, H. Chang, K. Folting, J. C. Huffman, G. Christou, D. N. Hendrickson, *J. Am. Chem. Soc.* **1987**, *109*, 5703 – 5711.

[15] S. Midollini, A. Orlandini, P. Rosa, L. Sorace, *Inorg. Chem.* **2005**, *44*, 2060 – 2066.

[16] SHELX-PC Package: Bruker Analytical X-ray Systems, Madison, WI, **1998**.

